(Received 16 June 2025, Accepted 11 July 2025, Scheduled 23 July 2025)

Wideband Metasurface Antenna with Polarization Reconfigurable Controlled by Resistors

Guanghuan Geng[1] and Zhendong Ding[2,*]

[1]Xuzhou Metro Group CO., LTD, Xuzhou 221000, China
[2]School of Electronic and Optical Engineering, Nanjing University of Science and Technology, Nanjing 210094, China

ABSTRACT: A polarization reconfigurable metasurface broadband antenna was proposed. A 2×2 metasurface was used to achieve circular polarization (CP) characteristics, and four resistors were embedded to achieve linear polarization (LP). Among them, characteristic mode analysis (CMA) was used to discover the CP characteristics of the metasurface. Adding resistors changed the direction of the mode current, which causes CP to switch to LP state. The design results were validated through fabrication and measurement. The measured results show that the impedance bandwidth (IBW) is 21.1%, the axial ratio bandwidth (ARBW) 12.9%, and the peak gain (PG) 7.7 dBic at 6.8 GHz in the CP state, its IBW 21.0%, and the PG 4.7 dBi at 7.0 GHz in the LP state. The proposed antenna has the characteristics of broadband, polarization reconfigurability, easy processing, and low cost, and its operating frequency can be used in the C-band of wireless communication.

1. INTRODUCTION

With the rapid development of satellite communication, remote sensing and telemetry, radar and radio, the demand and application scenarios of CP antenna are increasing [1–3]. Compared with LP antenna, CP antenna has many significant advantages. It can eliminate the loss caused by polarization distortion in communication, effectively reduce signal leakage, and resist the interference of natural factors. To meet the multifunctional requirements of the communication system, reconfigurable antenna has been studied by some scholars, which can realize the diversification of antenna performance [4, 5]. Reconfigurable antennas are divided into frequency reconfigurable [6–8], pattern reconfigurable [9–12], polarization reconfigurable [13–16], and hybrid reconfigurable [17–20] antennas. The emergence of reconfigurable antenna has played a positive role in promoting the performance improvement, cost compression, volume reduction, and mass reduction of the entire wireless communication system.

In terms of the reconfigurable antenna performance, polarization reconfiguration is flexible for receiving and transmitting signals. The methods to realize polarization reconfiguration are different, and the selection and location of devices are particularly important. In [13], an antenna is proposed, which uses six PIN diodes to achieve left-handed circular polarization (LHCP), right-handed circular polarization (RHCP), and LP. Switching between CP and LP can also be achieved with fewer PIN diodes, as [14]. In addition to the above, the dielectric resonator was applied in [15] and realized the conversion between vertical polarization (VP) and horizontal polarization (HP). An antenna using liquid metal flowing in the specified direction to realize the conversion among LHCP, RHCP, and LP is reported in [16]. Some hybrid reconfigurable antennas are also accompanied by polarization reconfiguration, such as simultaneous polarization and pattern reconfiguration in [17], simultaneous polarization and frequency reconfiguration in [18, 19], and simultaneous polarization, frequency, and pattern reconfiguration in [20]. For implementing polarization reconfiguration, diodes are most commonly used to achieve the orthogonal direction of current. The key to polarization reconfiguration is to change the direction of current at the appropriate location.

In this letter, a polarization-reconfigurable metasurface antenna with the wideband characteristic was studied. Firstly, a microstrip antenna was designed, incorporating metasurface to achieve CP, and CMA was used to analyze the mechanism of CP implementation on metasurface. Secondly, four resistors were loaded, and through CMA that they changed the orthogonal characteristics of the current, achieving LP. The proposed design can be converted between CP and LP. Finally, the feasibility of the proposed antenna design method is verified through antenna fabrication and measurement.

2. DESIGN AND ANALYSIS OF THE PROPOSED ANTENNA

2.1. Antenna Configuration

As illustrated in Fig. 1, the antenna includes a microstrip antenna substrate (F4B, $\varepsilon_r = 2.65$, $\tan\delta = 0.0015$) and a metasurface substrate (FR4, $\varepsilon_r = 4.4$, $\tan\delta = 0.02$). A radiation patch and a ground are respectively attached above and below the substrate, and a metasurface is attached above another substrate. Four resistors are loaded at the middle position between two metasurfaces to connect them. The connection between

* Corresponding author: Zhendong Ding (dingzhendong@njust.edu.cn).

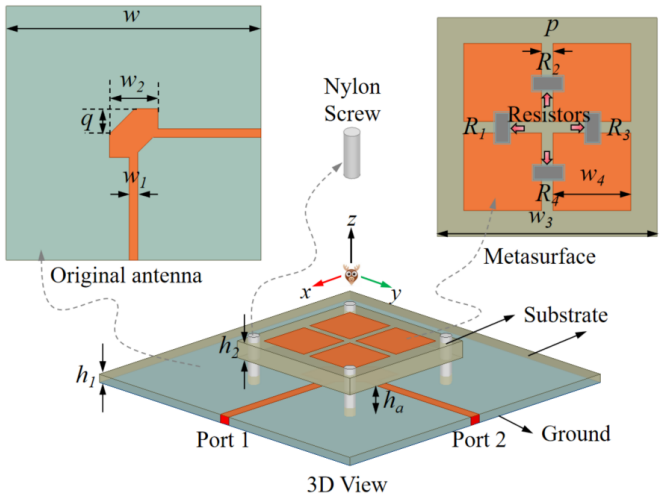

FIGURE 1. The exploded view of the polarization reconfigurable metasurface wideband antenna. The dimensions are ($w = 60$, $w_1 = 2$, $w_2 = 11.5$, $w_3 = 27$, $w_4 = 9.6$, $q = 14.4$, $w_6 = 6$, $p = 1$, $h_1 = 1$, $h_2 = 3$, and $h_a = 3$) [(Units: mm)].

the two substrate layers is fixed using nylon screws, and it is fed with a 50 Ω SMA.

2.2. The CP Mechanism of the Proposed Antenna

For rectangular microstrip antennas, the calculation of their radiation patch is shown in [21]. The calculated resonant frequency of antenna I is approximately 7.5 GHz. As shown in Figs. 2–3, the resonance effect of antenna I is not ideal. Consider implementing CP and chamfering antenna I, as shown in antenna II. The polarization effect of antenna II is better than that of antenna I, but it does not achieve the required performance. Antenna III has been distributed with right angled microstrip lines, and its resonance and polarization states are improved, but it does not achieve CP. To achieve CP, metasurfaces were introduced.

For metasurface, the CMA in [22, 23] is used to analyze antenna mechanisms. In CMA, the mode significance (MS) can discover the resonance potential of the structure. When MS $\geqslant 0.707$, it has the potential for resonance, physically defined as,

$$MS = 1/\left|1 + j\lambda_n\right| \tag{1}$$

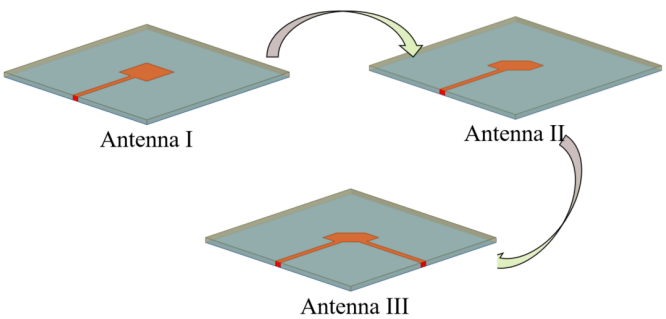

FIGURE 2. The evolution process of the microstrip antenna.

For symmetric metasurfaces, the condition for achieving CP is that the characteristic current direction is orthogonal. Furthermore, mode electric fields can be synchronized in phase or offset by 90°,

$$E_{x0} = E_{y0} \tag{2}$$

$$E_x(t) = E_{x0}\cos(\omega t + \varphi_x) \tag{3}$$

$$\begin{aligned} E_y(t) &= E_{y0}\cos(\omega t + \varphi_y \pm \pi/2 + 2n\pi) \\ &= \pm E_{x0}\sin(\omega t + \varphi_x) \end{aligned} \tag{4}$$

When $|E_{x0}| = |E_{y0}| = E_0$, the phases φ_x and φ_y are orthogonal and satisfy the relationship, indicating LHCP and RHCP,

$$\Delta\varphi = \varphi_x - \varphi_y = \begin{cases} +\pi/2(RHCP) \\ -\pi/2(LHCP) \end{cases} \tag{5}$$

Figure 4 shows the MS for mode analysis, where Mode 1 and Mode 2 coincide as the main mode. Its resonant bandwidth is 5.15–9.0 GHz, covering the resonant bandwidth of antenna III. Other modes played an auxiliary role in 6–7 GHz. Fig. 5 shows their characteristic currents, with the current directions of Mode 1 and Mode 2 being orthogonal. Fig. 6 shows the simulation results after loading the metasurface, with an IBW of 21.85% (6.66–8.29 GHz), an ARBW of 11.1% (7.08–7.91 GHz), a PG of 8.3 dBic, and the radiation efficiency (RE) greater than 80% within the resonant bandwidth. Its CMA verified that the addition of the metasurface enabled antennas to achieve the CP characteristic.

2.3. Analysis after Loading Resistors

Considering the change in polarization state, it is necessary to change the current directions of Mode 1 and Mode 2. Due to the difficulty in measuring and installing diodes and other devices, resistors are loaded between the metasurface units. Similarly, CMA was performed on the metasurface loaded with resistors to analyze its mechanism. As shown in Fig. 6, the MS changes significantly after loading resistors. The MSs of Modes 1, 2, 3, and 6 are significantly lower than 0.707, indicating no resonance potential. Mode 4 and Mode 5 only serve as auxiliary functions. However, the characteristic currents of Modes 1, 2, 3, and 6 become chaotic. Combining Fig. 7 and Fig. 8, the loading resistance changed from CP to LP. Fig. 9 shows the simulation comparison of loaded resistors. Its IBW hardly changes, and its gain increases with the increase of resistance value. Its ARBW is greater than 3 dB. Table 1 provides a comparison of simulation parameters for unloaded and loaded resistors.

From Fig. 9(a) and Table 1, it can be seen that the RE of the antenna is lower than that of the antenna without resistors. The reason is that resistors cause loss resistance, resulting in loss efficiency and a decrease in RE. Considering the gain, 151 Ω and 200 Ω are more suitable. In comparison, the efficiency and AR of 151 Ω are relatively stable.

3. MEASUREMENT OF THE PROPOSED ANTENNA

From design to simulation, to machining and measurement in Figs. 10–12, the feasibility of the designed antenna has been verified. The measurement shows two states: one without loaded resistors and the other with four resistors loaded.

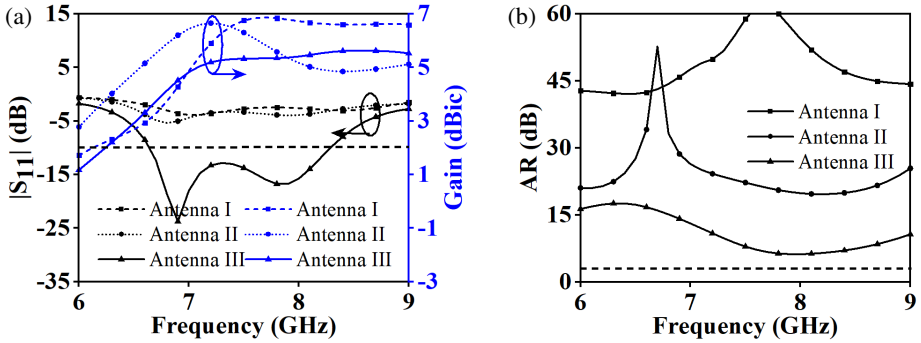

FIGURE 3. Simulation results of the evolution antennas: (a) $|S_{11}|$ and gain, (b) AR.

TABLE 1. Simulation results under resistors states.

Device	Value (Ω)	Pol.	AR BW (%)	IBW (%)	PG (dBi)	RE (%)
No	No	No	11.1	21.8	8.3	82.1–87.7
Resistors	51	LP	/	22.4	3.0	55.6–68.9
	100	LP	/	22.3	4.1	60.1–65.6
	151	LP	/	22.2	4.8	61.4–65.2
	200	LP	/	22.1	5.5	60.0–68.1

TABLE 2. Comparison of the antenna's performances (N. A: Not applicable).

Ref.	Profile (λ_0)	ARBW (%)	IBW (%)	PG (dBi)	Max. RE (%)	PINs/Resistors/ Capacitances/ Inductances	Reconfigurable type
2024/[6]	0.03	1.5 (RHCP) 1.6 (RHCP)	5.1 (RHCP) 6.2 (RHCP)	4.40 4.80	90.0	2 capacitances	Frequency
2023/[9]	0.08	N. A	9.3 8.2	7.15 3.94	N. A	2 PINs	Pattern
2024/[13]	0.04	11.2	11.7 (CP) 11.6 (LP)	4.20 5.35	N. A	4 PINs and 3 inductances	Polarization
2021/[15]	0.21	N. A	18.1 (HP) 16.8 (VP)	2.04 1.10	70.8	Dielectric resonator	Polarization
2021/[17]	0.07	30.0	21.0 (HP) 22.0 (VP)	3.66 4.38	N. A	16 PINs	Polarization and pattern
This work	0.17	12.9	21.1 (CP) 21.0 (LP-R)	7.70 4.70	87.7 65.2	4 resistors	Polarization

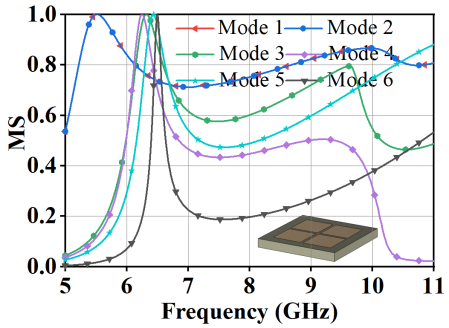

FIGURE 4. The MS of the metasurface.

When no resistor is loaded, its IBW ($|S_{11}|$) is 6.62–8.18 GHz (21.1%), its IBW ($|S_{22}|$) 6.60–8.30 GHz (22.8%), its ARBW 7.01–7.98 GHz (12.9%), and its PG 7.7 dBic at 6.8 GHz. When four resistors are loaded, the polarization state is CP to LP. A resistance value of 151 Ω was selected for measurement, with an IBW of 6.60–8.15 GHz (21.0%) and a PG of 4.7 dBi at 7.0 GHz.

Figure 13 shows the radiation patterns of LHCP and RHCP at 7.4 GHz and 7.6 GHz. The proportion of LHCP is relatively high near 0°, while RHCP is relatively high in other areas, especially around 180°. Both LHCP and RHCP exhibit radiation phenomena. Compared to 7.4 GHz, LHCP is offset by 5°–10° at 7.6 GHz. Fig. 14 shows the radiation pattern after loading

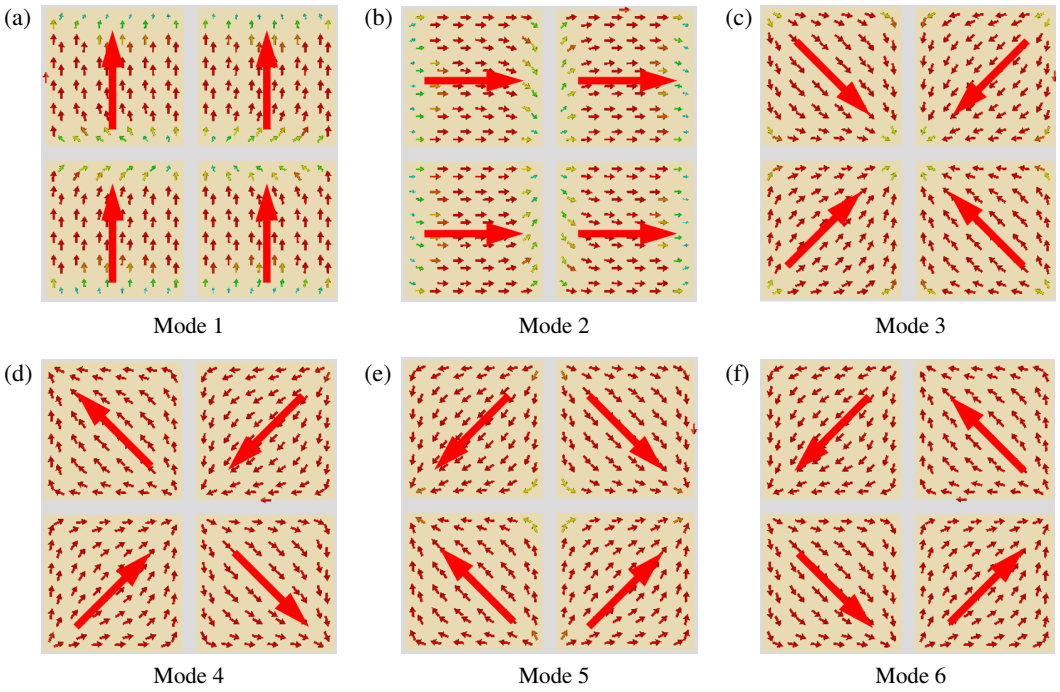

FIGURE 5. Characteristic currents of an unloaded resistors metasurface.

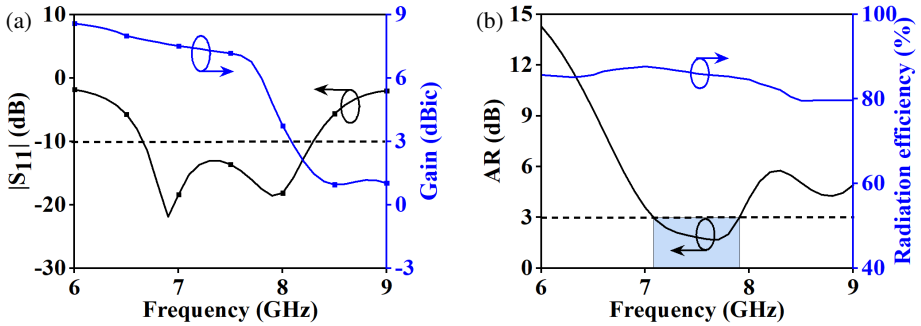

FIGURE 6. Simulation results of metasurface broadband CP antenna: (a) $|S_{11}|$ and gain, (b) AR and RE.

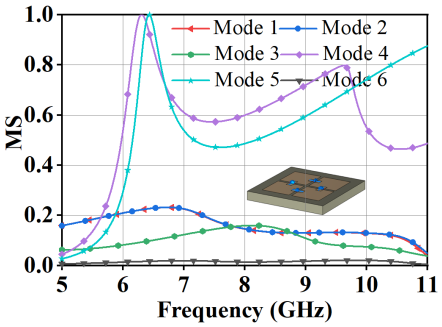

FIGURE 7. The MS of the metasurface after loading resistors.

four resistors. Both the E and H planes have offset phenomena, which do not affect the radiation performance of the antenna. Overall, measurement errors exist due to the assembly and welding of the antenna, but the consistency between simulation and measurement meets the requirements. Table 2 compares the performance of several antennas. The profiles of [6, 9, 13] are lower than the proposed antenna, but their bandwidth is relatively narrow. The profile of [15] is high; the bandwidth is narrow; the gain is low. The profile of [17] is low, and the ARBW is wide, but the low gain and 16 diodes make antenna measurements more complex (The solid line represents simulation, and the dashed line represents measurement.)

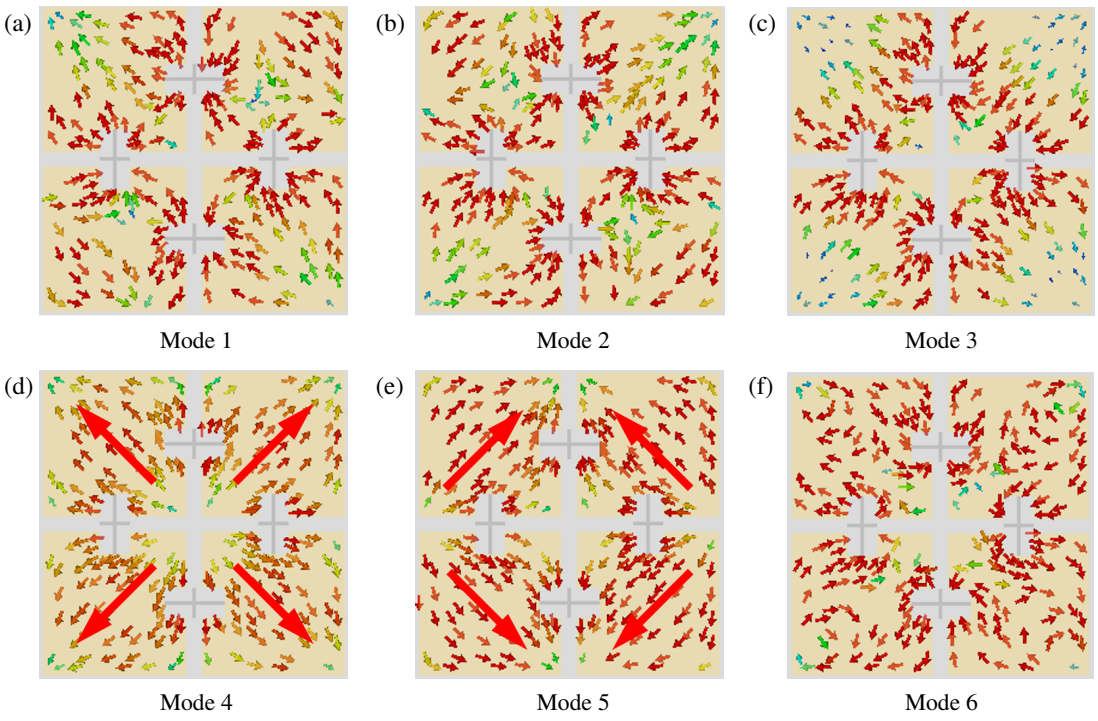

FIGURE 8. Characteristic currents of metasurface after loading resistors.

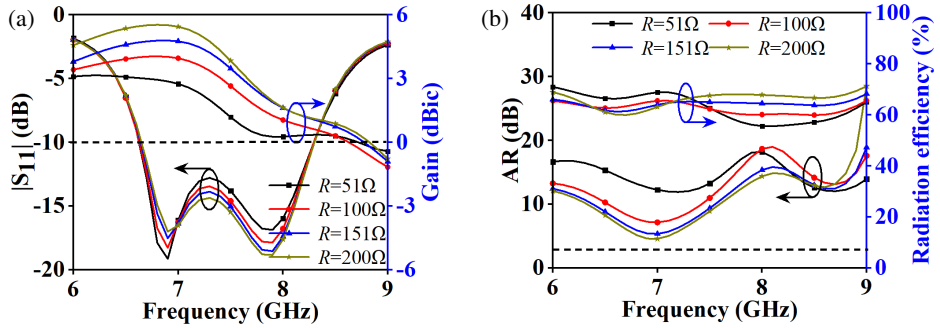

FIGURE 9. Simulation comparison results of the antenna after loading resistors: (a) $|S_{11}|$ and gain, (b) AR and RE.

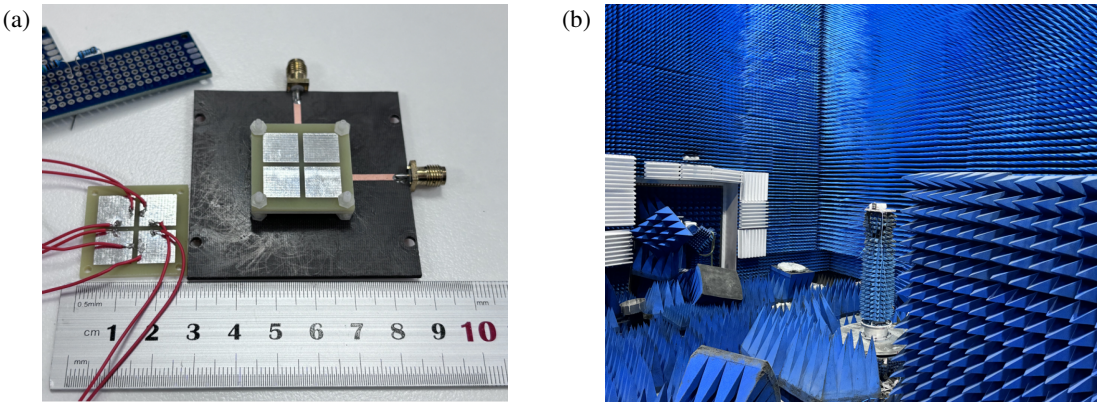

FIGURE 10. Prototype and measurement: (a) Fabricated antenna, and (b) the anechoic chamber for measurement.

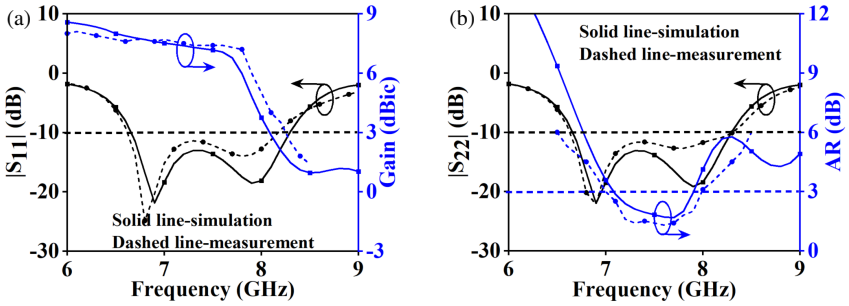

FIGURE 11. The simulated and measured results when no resistor is loaded: (a) $|S_{11}|$ and gain, and (b) $|S_{22}|$ and AR.

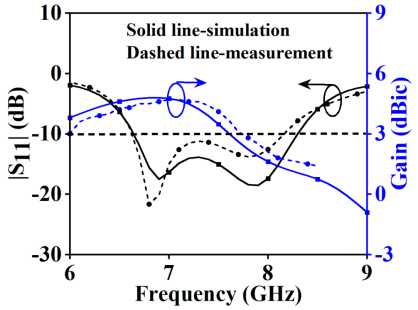

FIGURE 12. The simulated and measured results when resistors are loaded (151 Ω): $|S_{11}|$ and gain.

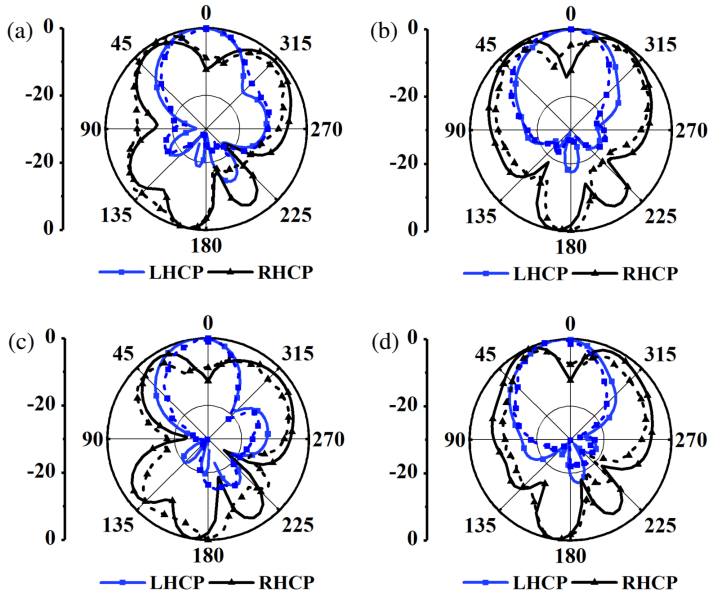

FIGURE 13. The simulated and measured radiation patterns when no resistor is loaded: (a) xoz plane at 7.4 GHz, (b) yoz plane at 7.4 GHz, (c) xoz plane at 7.6 GHz, (d) yoz plane at 7.6 GHz.

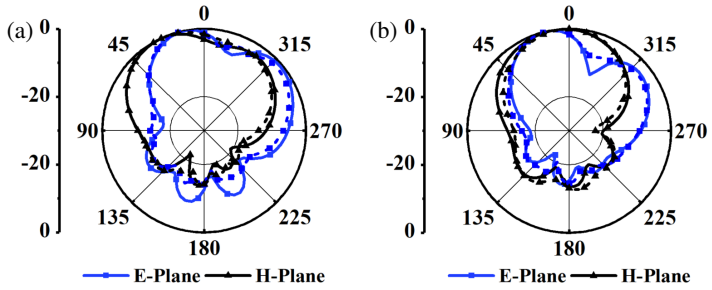

FIGURE 14. The simulated and measured radiation patterns when resistors are loaded: (a) E and H-plane at 7.0 GHz, (b) E and H-plane at 7.5 GHz.

4. CONCLUSION

A metasurface broadband polarization reconfigurable antenna has been proposed. The proposed innovative antenna uses resistors to switch between CP and LP. CMA was used to analyze the CP mechanism of the metasurface. After loading resistors, the direction of current was blocked, achieving LP. Its key performance advantages include broadband, switching between two polarizations, simple structure, and low cost. This antenna can be used in the C-band (4 GHz to 8 GHz) for wireless communication.

ACKNOWLEDGEMENT

This work was supported in part by the Postgraduate Research & Practice Innovation Program of Jiangsu Province in China (KYCX23_0467).

REFERENCES

[1] Gu, W. D. and Y. Zhang, "A type of dual/circularly-polarized filtering dipole antenna design based on coupled lines," *IEEE Antennas and Wireless Propagation Letters*, Vol. 24, No. 2, 489–493, Feb. 2025.

[2] Sun, X.-Y., B. Wu, H.-H. Zhang, K.-X. Guo, H.-Y. Xie, X.-Z. Song, and T. Su, "Ultrawideband circularly polarized halved-type Vivaldi antenna with symmetrical radiation pattern," *IEEE Antennas and Wireless Propagation Letters*, Vol. 23, No. 2, 633–637, Feb. 2024.

[3] Zhang, L., J.-W. Liu, B. Chen, L.-Y. Yi, D. Liu, Z.-B. Weng, and Y.-C. Jiao, "A dual-port dual-wideband dual-sense circularly polarized DRA with a novel feeding mechanism," *IEEE Open Journal of Antennas and Propagation*, Vol. 6, No. 1, 229–234, Feb. 2025.

[4] Li, T., H. Zhai, X. Wang, L. Li, and C. Liang, "Frequency-reconfigurable bow-tie antenna for Bluetooth, WiMAX, and WLAN applications," *IEEE Antennas and Wireless Propagation Letters*, Vol. 14, 171–174, 2015.

[5] Cai, Y.-M., S. Gao, Y. Yin, W. Li, and Q. Luo, "Compact-size low-profile wideband circularly polarized omnidirectional patch antenna with reconfigurable polarizations," *IEEE Transactions on Antennas and Propagation*, Vol. 64, No. 5, 2016–2021, May 2016.

[6] Han, S., Z. Wang, and Y. Dong, "Miniaturized circularly polarized reconfigurable capacitance-loaded patch antenna," *IEEE Antennas and Wireless Propagation Letters*, Vol. 23, No. 4, 1226–1230, Apr. 2024.

[7] Li, J., B. Wu, J. Zhou, C. Fan, and Y. Liu, "Impedance regulation of graphene-loaded branch for frequency-reconfigurable antenna with enhanced radiation efficiency," *IEEE Antennas and Wireless Propagation Letters*, Vol. 23, No. 3, 1065–1069, Mar. 2024.

[8] Chen, Z., H.-Z. Li, H. Wong, W. He, J. Ren, and T. Yuan, "A frequency-reconfigurable dielectric resonator antenna with a water layer," *IEEE Antennas and Wireless Propagation Letters*, Vol. 22, No. 6, 1456–1460, Jun. 2023.

[9] Tan, S., Y. Xiao, Y. Liu, Z. Liang, Y. Li, and S. Xu, "A pattern-reconfigurable endfire antenna based on compact folded slot with vertical polarization," *IEEE Antennas and Wireless Propagation Letters*, Vol. 22, No. 7, 1537–1541, Jul. 2023.

[10] Yuan, W., J. Huang, X. Zhang, K. Cui, W. Wu, and N. Yuan, "Wideband pattern-reconfigurable antenna with switchable monopole and Vivaldi modes," *IEEE Antennas and Wireless Propagation Letters*, Vol. 22, No. 1, 199–203, Jan. 2023.

[11] Huang, T.-G., F.-C. Chen, K.-R. Xiang, L.-Y. Wei, and W.-F. Zeng, "Pattern reconfigurable cavity-backed antenna based on radiant metal blocks," *IEEE Antennas and Wireless Propagation Letters*, Vol. 23, No. 12, 4553–4557, Dec. 2024.

[12] Zhang, F., L. Liu, Y. Zhang, and F. Zhang, "Compact ultrathin wideband pattern-reconfigurable antenna with enhanced operating bandwidth," *IEEE Antennas and Wireless Propagation Letters*, Vol. 23, No. 12, 4443–4447, Dec. 2024.

[13] Jaiswal, R. K., Aakash, A. K. Ojha, C.-Y.-D. Sim, and K. V. Srivastava, "Wideband low-profile endfire antenna with polarization reconfigurability," *IEEE Transactions on Circuits and Systems II: Express Briefs*, Vol. 71, No. 4, 1984–1988, Apr. 2024.

[14] Nguyen-Dinh, T., H. Nguyen-Tuan, H. Tran-Huy, D. Nguyen-Quoc, and N. Nguyen-Trong, "A simple polarization-reconfigurable series-fed patch array using switchable feeding network," *IEEE Antennas and Wireless Propagation Letters*, Vol. 23, No. 9, 2658–2662, Sep. 2024.

[15] Liu, X., K. W. Leung, and N. Yang, "Wideband horizontally polarized omnidirectional cylindrical dielectric resonator antenna for polarization reconfigurable design," *IEEE Transactions on Antennas and Propagation*, Vol. 69, No. 11, 7333–7342, Nov. 2021.

[16] Xing, H., C. Tang, Z. Li, M. Wang, C. Fan, H. Zheng, and E. Li, "Three-polarization-reconfigurable antenna array implemented by liquid metal," *IEEE Antennas and Wireless Propagation Letters*, Vol. 23, No. 1, 374–378, Jan. 2024.

[17] Li, W., Y. M. Wang, Y. Hei, B. Li, and X. Shi, "A compact low-profile reconfigurable metasurface antenna with polarization and pattern diversities," *IEEE Antennas and Wireless Propagation Letters*, Vol. 20, No. 7, 1170–1174, Jul. 2021.

[18] Liu, Y., Q. Wang, Y. Jia, and P. Zhu, "A frequency- and polarization-reconfigurable slot antenna using liquid metal," *IEEE Transactions on Antennas and Propagation*, Vol. 68, No. 11, 7630–7635, Nov. 2020.

[19] Liu, M., S. Chen, Z. Zhao, H. Chu, P. Xiao, and G. Li, "A polarization-and frequency-reconfigurable transparent liquid antenna," *IEEE Antennas and Wireless Propagation Letters*, Vol. 23, No. 8, 2281–2285, Aug. 2024.

[20] Rodrigo, D., B. A. Cetiner, and L. Jofre, "Frequency, radiation pattern and polarization reconfigurable antenna using a parasitic pixel layer," *IEEE Transactions on Antennas and Propagation*, Vol. 62, No. 6, 3422–3427, Jun. 2014.

[21] Wang, H., X. B. Huang, and D. G. Fang, "A single layer wideband U-slot microstrip patch antenna array," *IEEE Antennas and Wireless Propagation Letters*, Vol. 7, 9–12, 2008.

[22] Ding, Z., J. Li, J. Cao, H. Wang, M. Y.-W. Chia, and N. Nasimuddin, "Wideband dual-polarized metasurface antenna with polarization reconfigurable controlled by diode and resistor, featuring low RCS," *IEEE Antennas and Wireless Propagation Letters*, Vol. 24, No. 5, 1208–1212, May 2025.

[23] Wang, Y., Z. Ding, J. Yu, J. Cao, H. Wang, M. Y.-W. Chia, and N. Nasimuddin, "Metasurface-based circularly polarised antenna: Enhanced bandwidth with characteristic mode analysis and symmetric branch design," *IET Microwaves, Antennas & Propagation*, Vol. 18, No. 12, 974–984, 2024.